STRUCTURAL CONTROL AND HEALTH MONITORING
Struct. Control Health Monit. 2006; **13**:245–259
Published online 19 December 2005 in Wiley InterScience (www.interscience.wiley.com). DOI: 10.1002/stc.139

Health monitoring for strongly non-linear systems using the Ensemble Kalman Filter

R. Ghanem[1,*,†] and G. Ferro[2]

[1] *University of Southern California, 210 KAP, Los Angeles, CA 90089, U.S.A.*
[2] *University of Messina, Salita Sperone, 31, 98166 Messina, Italy*

SUMMARY

Many structural engineering problems of practical interest involve pronounced non-linear dynamics the governing laws of which are not always clearly understood. Standard identification and damage detection techniques have difficulties in these situations which feature significant modelling errors and strongly non-Gaussian signals. This paper presents a combination of the ensemble Kalman filter and non-parametric modelling techniques to tackle structural health monitoring for non-linear systems in a manner that can readily accommodate the presence of non-Gaussian noise. Both location and time of occurrence of damage are accurately detected in spite of measurement and modelling noise. A comparison between ensemble and extended Kalman filters is also presented, highlighting the benefits of the present approach. Copyright © 2005 John Wiley & Sons, Ltd.

KEY WORDS: ensemble Kalman filter; parameter identification; damage detection; reduced-order models

1. INTRODUCTION

Technologies, such as sensors and microprocessors, supporting health monitoring of civil structures and infrastructure have been advancing rapidly, in the process alleviating many of the challenges associated with implementing these monitoring systems. For instance issues of displacement measurements, spatially distributed measurements, and networked sensors have been alleviated if not completely resolved. A significant difficulty remains that is associated with the physical complexity of the systems comprising these structures. Mathematical models representing these systems incur significant uncertainties to the point that any health monitoring algorithm that is not very robust with respect to modelling errors is likely to fail in a practical setting. Moreover, in the presence of non-linearities associated with post-damage behaviour, it

*Correspondence to: R. Ghanem, University of Southern California, 210 KAP, 3620 S. Vermont St., Los Angeles, CA 90089, U.S.A.
† E-mail: ghanem@usc.edu

Contract/grant sponsor: NSF; contract/grant number: DMS-0512231

Received 30 May 2005
Revised 6 September 2005

can be expected that the statistical description of many of the signals involved in the monitoring process will deviate significantly from the Gaussian prototype assumed in most current procedures. This again presents a challenge to many current identification and health monitoring algorithms. These challenges notwithstanding, this has been a very active research area, specially over the past decade [1–6].

Broadly, identification methods can be grouped according to whether they process information in the frequency or the time domain. In the frequency domain, indices of performance are usually obtained from estimates of natural frequencies, damping ratios and mode shapes. These methods, in general, cannot capture sharp changes occurring over short time intervals, as is the case with structural damage taking place in the course of an extreme event. The time domain methods, on the other hand, permit a recursive estimation of the parameters, and are thus well-positioned to detect significant changes in the structure. Many of these methods are based, either implicitly or explicitly, on least squares minimization concepts [7–9]. One of the most significant recursive algorithms involves various approaches based on the Kalman filter [10, 11]. These approaches integrate a predictive phase with a corrective phase to assimilate measurements as they are taken. Non-recursive time-domain methods have also been proposed and developed that rely on Galerkin projections, and where the whole time series is analysed at once. In particular, methods that combine Galerkin schemes with wavelet expansions have been successful at this task [12, 13].

A method is reviewed and applied in this paper that extends the Kalman filtering approach to problems involving non-Gaussian and non-linear dynamics that cannot be linearized. Specifically, these ensemble Kalman filtering approaches, have been developed for geophysical applications and have proven to be very robust in the presence of significant modelling and measurement errors [14–17]. This ensemble Kalman filtering approach is coupled, in this paper, to a non-parametric model of the non-linearities in the system [18] thus providing robustness against missing dynamics and other modelling errors.

The next section provides a brief overview of the Kalman filter together with its relation to the extended Kalman filter (ExKF) and the ensemble Kalman filter (EnKF). Following that, implementation issues of the EnKF are described before, finally, the method is demonstrated by its application to the detection of a degrading hysteretic element in a multistorey building.

2. FROM THE KALMAN FILTER TO THE EXTENDED AND ENSEMBLE KALMAN FILTER

Starting with a brief overview of the standard Kalman filter (KF), this section presents its extension towards the ExKF and to the EnKF forms, respectively.

The KF addresses the general problem of estimating the state $\mathbf{\Psi}$ of a time controlled process the evolution of which is governed by a linear difference equation. The model is driven by a stochastic process. The filter enables the estimations of past, present, and future states, and is somewhat robust to modelling errors. In addition to providing estimates of the state, the KF permits the evaluation of the error covariance. The Kalman filter works using a two-step cycle: (1) In the first cycle, the *predictor* phase, the current (at time instant k) state estimate $\mathbf{\Psi}^{(k/k)}$ and error covariance $\mathbf{P}^{(k/k)}$ are projected ahead in time, using the system model resulting in the *a priori* estimate for the next time step $\mathbf{\Psi}^{(k+1/k)}$ and $\mathbf{P}^{(k+1/k)}$; (2) in the second cycle, the corrector, or *filtering* phase, the projected estimate is adjusted using actual measurements $\mathbf{d}$ at time instant

$k+1$, resulting in an improved *a posteriori* estimate ($\Psi^{(k+1/k+1)}$ and $P^{(k+1/k+1)}$), for both state and error covariance, respectively. The two phases are briefly reviewed next.

Predictor phase: Consider a dynamical system, characterized at any instant of time, k, by an n-dimensional state vector. This state vector could either refer to a physical constraint on the description of a continuum system or can be induced by a numerical discretization process. Denote by $\mathbf{F}$ the operator that characterizes the transition between successive states. For linear time-invariant finite-dimensional systems, $\mathbf{F}$ is thus represented by a time invariant $n \times n$ transition matrix. The predicted state vector is propagated from the current state vector using this transition operator in the form

$$\boldsymbol{\Psi}^{(k+1/k)} = \mathbf{F}\boldsymbol{\Psi}^{(k/k)} + \mathbf{w}^{(k)}, \quad \boldsymbol{\Psi}^{(k/k)}, \boldsymbol{\Psi}^{(k+1/k)}, \mathbf{w}^{(k)} \in \mathbb{R}^n, \quad \mathbf{F} \in \mathbb{R}^{n\times n} \tag{1}$$

where n is the dimension of the state vector $\boldsymbol{\Psi}^{(k/k)}$ at time k, and $\mathbf{w}$ is a Gaussian vector white noise reflecting the possibility of modelling errors. Using Equation (1) as the definition of the predicted state, it is possible to define *a priori* and *a posteriori* errors as

$$\mathbf{e}^{(k+1/k)} = \boldsymbol{\Psi}_t^{k+1} - \boldsymbol{\Psi}^{(k+1/k)}, \quad \mathbf{e}^{(k+1/k+1)} = \boldsymbol{\Psi}_t^{k+1} - \boldsymbol{\Psi}^{(k+1/k+1)}$$
$$\mathbf{e}^{(k+1/k)}, \mathbf{e}^{(k+1/k+1)}, \boldsymbol{\Psi}_t^{k} \in \mathbb{R}^n \tag{2}$$

where $\boldsymbol{\Psi}_t^k$ denotes the true state vector at instant k. The *a priori* and *a posteriori* error covariance matrices are defined, respectively, as

$$\mathbf{P}^{(k+1/k)} = E[\mathbf{e}^{(k+1/k)}e^{(k+1/k)^{\mathrm{T}}}], \quad \mathbf{P}^{(k+1/k+1)} = E[\mathbf{e}^{(k+1/k+1)}e^{(k+1/k+1)^{\mathrm{T}}}]$$
$$\mathbf{P}^{(k+1/k)}, \mathbf{P}^{(k+1/k+1)} \in \mathbb{R}^{n\times n} \tag{3}$$

In light of the variance minimization implicit in the KF, the error covariance matrix is projected forward in time according to the following equation:

$$\mathbf{P}^{(k+1/k)} = \mathbf{F}\mathbf{P}^{(k/k)}\mathbf{F}^{\mathrm{T}} + \mathbf{Q} \tag{4}$$

where the $n \times n$ matrix $\mathbf{Q}$ is the covariance matrix for the model errors, $\mathbf{w}$. Equations (1) and (4) describe the evolution in time of $\boldsymbol{\Psi}^{(k+1/k)}$ and $\mathbf{P}^{(k+1/k)}$.

2.1. Filtering phase

The filtering step in the KF provides an update to the predictions whenever observations are made available. The filtered values of $\boldsymbol{\Psi}^{(k+1/k+1)}$ and $\mathbf{P}^{(k+1/k+1)}$ can be shown to be given by [10],

$$\boldsymbol{\Psi}^{(k+1/k+1)} = \boldsymbol{\Psi}^{(k+1/k)} + \mathbf{K}(\mathbf{d}^{(k+1)} - \mathbf{H}\boldsymbol{\Psi}^{(k+1/k)}) \tag{5}$$

and

$$\mathbf{P}^{(k+1/k+1)} = (\mathbf{I} - \mathbf{K}\mathbf{H})\mathbf{P}^{(k+1/k)} \quad \mathbf{I}, \mathbf{K}, \mathbf{H} \in \mathbb{R}^{n\times n} \tag{6}$$

where I is the identity matrix and K is the Kalman gain defined as

$$\mathbf{K} = \mathbf{P}^{(k+1/k)}\mathbf{H}^{\mathrm{T}}(\mathbf{H}\mathbf{P}^{(k+1/k)}\mathbf{H}^{\mathrm{T}} + \mathbf{R})^{-1} \tag{7}$$

where $\mathbf{R}$ is the error covariance matrix for measurement noise, $\mathbf{H}$ is the measurement operator relating the true model state to the m-dimensional observation vector $\mathbf{d}$. Measurement noise are

included in the form of vector $\boldsymbol{\gamma}$, according to the linear observation equation,

$$\mathbf{d} = \mathbf{H}\boldsymbol{\Psi}^t + \boldsymbol{\gamma} \tag{8}$$

2.2. Extended Kalman filter

The filtering equations for the state and error covariance, presented above, depend on the assumption of model linearity. Extensions to non-linear dynamics can be readily accommodated through a linearization process. This has proven most useful for situations where system parameters are appended to the state vector, the foregoing procedure enabling the use of Kalman filtering as a recursive parameter estimation framework. Thus, if the state vector is governed by a non-linear model, Equation (1) can be replaced by the following equation:

$$\boldsymbol{\Psi}^{(k+1/k)} = \mathbf{f}(\boldsymbol{\Psi}^{(k/k)}) + \mathbf{w}^{(k)} \quad \mathbf{f} \in \mathbb{R}^n \tag{9}$$

By linearizing the function $\mathbf{f}(\boldsymbol{\Psi})$ around the most recent estimate of the state, equations associated with the Kalman filter can be applied, resulting in approximations to both the state and the error covariance. Defining the operator $\mathbf{F}$ has been defined as the linearized version of $\mathbf{f}$, the error covariance is given by a similar equation to (4), and the filtering phase retains the same formulation.

2.3. Ensemble Kalman filter

In both KF and ExKF, the theoretical derivation of filtering equations rely on the simple structure of linear dynamical systems excited by Gaussian noise, recognizing that the ensuing dynamics is also Gaussian. In situations where either the noise is significantly non-Gaussian or the dynamics is highly non-linear, the accuracy associated with filtering the linearized system may not be acceptable. The analysis scheme proposed in the EnKF [14] addresses this difficulty. It is relevant to note that the EnKF can be viewed as a particular variation on the more general class of approaches referred to as interacting particle systems or particle filtering [19]. EnKF relies on the traditional corrector equation of the standard Kalman filter, except that the gain is calculated from the error covariances provided by the ensemble of model states. This provides for the effect of non-linear dynamics on the statistics of the state. The ensemble error covariance matrix used in the Kalman gain is thus evaluated as

$$\mathbf{P} \approx \mathbf{P}_e = \overline{(\boldsymbol{\Psi} - \bar{\boldsymbol{\Psi}})(\boldsymbol{\Psi} - \bar{\boldsymbol{\Psi}})^{\mathrm{T}}} \tag{10}$$

where the overbar denotes the operator of ensemble averaging. It is essential to note that the observations are treated as random variables defining an ensemble of observations in the form

$$\mathbf{d}_j = \mathbf{d} + \boldsymbol{\gamma}_j, \quad j = 1, \ldots, N, \quad \mathbf{d}_j, \gamma_j \in \mathbb{R}^m \tag{11}$$

where N is the cardinality of the ensemble. The error covariance matrix of the measurements is obtained from the ensemble as

$$\mathbf{R}_e = \overline{\boldsymbol{\gamma}\boldsymbol{\gamma}^{\mathrm{T}}} \quad \gamma \in \mathbb{R}^{m \times N}, \quad \mathbf{R}_e \in \mathbb{R}^{m \times m} \tag{12}$$

The filtering is performed by Equation (5) on each member of the ensemble,

$$\boldsymbol{\Psi}^{(k+1/k+1)} = \boldsymbol{\Psi}^{(k+1/k)} + \mathbf{K}(\mathbf{d}_j^{(k+1)} - \mathbf{H}\boldsymbol{\Psi}_j^{(k+1/k)}) \tag{13}$$

using the gain,

$$\mathbf{K} = \mathbf{P}_e^{(k+1/k)}\mathbf{H}^{\mathrm{T}}(\mathbf{H}\mathbf{P}_e^{(k+1/k)}\mathbf{H}^{\mathrm{T}} + \mathbf{R}_e)^{-1} \tag{14}$$

Clearly, in light of definition (10), it is not necessary to update the matrix $\mathbf{P}_e$.

3. PRACTICAL IMPLEMENTATION OF THE ENSEMBLE KALMAN FILTER

In the following the particular implementation of the EnKF used in this paper is briefly described. Consider the signal to be tracked, assumed to be governed by the stochastic difference predictor equation,

$$\mathbf{\Psi}_i^{(k+1/k)} = \mathbf{f}(\mathbf{\Psi}_i^{(k/k)}) = \mathbf{w}_i^{(k/k)} \tag{15}$$

where $\mathbf{\Psi}_i^{(k/k)}$ is the state vector at time k for the ith ensemble member and $\mathbf{w}_i$ is the process noise vector perturbing the ith ensemble member. Once the state vectors $\mathbf{\Psi}_i$ (when confusion can be avoided, superscript are dropped for clarity) have been estimated, the following matrix can be evaluated:

$$\mathbf{A} = (\mathbf{\Psi}_1, \ldots, \mathbf{\Psi}_N) \in \mathbb{R}^{n\times N} \tag{16}$$

where n is the number of state variables and N is the number of ensemble members. Defining $\mathbf{1}_N$ as the $N \times N$ matrix having each element equal to $1/N$, it is possible to define the ensemble mean matrix as

$$\bar{\mathbf{A}} = \mathbf{A}\mathbf{1}_N, \quad \bar{\mathbf{A}} \in \mathbb{R}^{n\times N} \tag{17}$$

Similarly, an ensemble perturbation matrix is defined as

$$\mathbf{A}' = \mathbf{A} - \bar{\mathbf{A}} = \mathbf{A}(\mathbf{I} - \mathbf{1}_N), \quad \mathbf{A}' \in \mathbb{R}^{n\times N} \tag{18}$$

Now it is possible to define the ensemble covariance matrix around the ensemble mean as

$$\mathbf{P}_e = \frac{1}{N-1}\mathbf{A}'\mathbf{A}'^{\mathrm{T}}, \quad \mathbf{P} \in \mathbb{R}^{n\times n} \tag{19}$$

In implementing the filtering phase, consider the vector of measurements, $\mathbf{d} \in \mathbb{R}^m$, expressed in the form

$$\mathbf{d} = \mathbf{H}\mathbf{\Psi}_t \tag{20}$$

where $\mathbf{H}$ is the measurement operator relating the true model state to the observations, $\mathbf{\Psi}_t$ is the true model state vector and m is the number of measurements. The N vectors of observations can thus be defined as

$$\mathbf{d}_j = \mathbf{d} + \boldsymbol{\gamma}_j, \quad j = 1, \ldots, N \tag{21}$$

which can be conveniently aggregated into the following form:

$$\mathbf{D} = (\mathbf{d}_1, \ldots, \mathbf{d}_N) \quad \mathbf{D} \in \mathbb{R}^{m\times N} \tag{22}$$

Moreover defining the following matrix:

$$\boldsymbol{\gamma} = (\boldsymbol{\gamma}_1, \ldots, \boldsymbol{\gamma}_N), \quad \boldsymbol{\gamma} \in \mathbb{R}^{m\times N} \tag{23}$$

the error covariance matrix of the measurements can be expressed as

$$\mathbf{R}_e = \frac{1}{N-1}\boldsymbol{\gamma}\boldsymbol{\gamma}^{\mathrm{T}}, \quad \mathbf{R}_e \in \mathbb{R}^{m\times m} \tag{24}$$

It is then possible to define the corrector equation as

$$\mathbf{A}^a = \mathbf{A} + \mathbf{P}_e\mathbf{H}^{\mathrm{T}}(\mathbf{H}\mathbf{P}_e\mathbf{H}^{\mathrm{T}} + \mathbf{R}_e)^{-1}(\mathbf{D} - \mathbf{K}\mathbf{A}) \tag{25}$$

where $\mathbf{H}$ is the measurement operator relating the true model state to the observations, and $\mathbf{A}$ is the matrix holding in its columns all filtering estimate state vectors.

4. APPLICATION TO STRUCTURAL HEALTH MONITORING

Both the ExKF and the EnKF can be adapted to the recursive estimation of model parameters. However, it is clear from its formulation that for strongly non-linear systems, the EnKF can be expected to have superior performance over the ExKF. It is the object of this paper to demonstrate the efficacy of the EnKF to problems in structural health monitoring, and in particular to situations that, while common in practice, cannot be readily treated using the ExKF in view of the non-linearities involved.

Specifically, consider the frame structure depicted in Figure 1(a). This is a model of a four-storey shear building, with constant stiffness on each floor and 5% damping ratio in all modes. The input excitation is taken as a horizontal ground motion described by a sinusoidal wave. All structural elements of this frame are assumed to involve hysteretic behaviour, and it is supposed that, because of damage, an instantaneous change of the hysteretic loop occurs in one element, namely that corresponding to the first floor. Of great interest is the localization of damage in both space and time and also the tracking of the state of the system throughout and subsequent to the evolution of damage. Both the EnKF and the ExKF are applied to this problem. A dataset representing measurements of displacements and velocities at each floor, has been synthesized numerically by representing the hysteretic restoring force according to the Bouc-Wen model [20], which is therefore assumed to be the 'exact' model for the present hysteretic behaviour. The equation of motion of the system with this type of hysteresis can be written as

$$\mathbf{M}\ddot{\mathbf{u}}(t) + \mathbf{C}\dot{\mathbf{u}}(t) + \alpha\mathbf{K}_{\mathrm{el}}\mathbf{u}(t) + (1-\alpha)\mathbf{K}_{\mathrm{in}}\mathbf{z}(\mathbf{x},t) = -\mathbf{M}\boldsymbol{\tau}\ddot{u}_g(t) \tag{26}$$

where $\mathbf{M}$, $\mathbf{C}$, $\mathbf{K}_{\mathrm{el}}$ and $\mathbf{K}_{\mathrm{in}}$ are the mass, damping, elastic and inelastic stiffnesses, respectively; α is the ratio between the post-yielding stiffness and the elastic stiffness (considered for simplicity to be constant for each floor), $\boldsymbol{\tau}$ is an influence vector, $\mathbf{u}$ is the displacement vector, $\mathbf{x}$ is the inter-storey drift vector and $\mathbf{z}$ is the n-dimensional evolutionary hysteretic vector whose ith component is represented by the Bouc-Wen model as

$$z_i = A_i\dot{x}_i - \beta_i \mid \dot{x}_i \mid\mid z_i \mid^{n_i-1} z_i - \gamma_i\dot{x}_i \mid z_i \mid^{n_i}, \quad i = 1,\ldots,n \tag{27}$$

Defining the $3n$-dimensional state vector $\mathbf{Y} = [\mathbf{u}\ \dot{\mathbf{u}}\ \mathbf{z}]$, the state space representation of Equation (26) is given as

$$\dot{\mathbf{Y}} = \mathbf{f}(\mathbf{Y}) + \mathbf{G}\ddot{u}_g \tag{28}$$

where $\mathbf{G}$ is an influence matrix, and $\mathbf{f}(\mathbf{Y})$ is the following $3n$-dimensional vector:

$$\mathbf{f}(\mathbf{Y}) = [\dot{\mathbf{u}} \quad -\mathbf{M}^{-1}(\mathbf{C}\dot{\mathbf{u}} + \alpha\mathbf{K}\mathbf{u} + (1-\alpha)\mathbf{K}\mathbf{z})\ \ \mathbf{z}]^{\mathrm{T}} \tag{29}$$

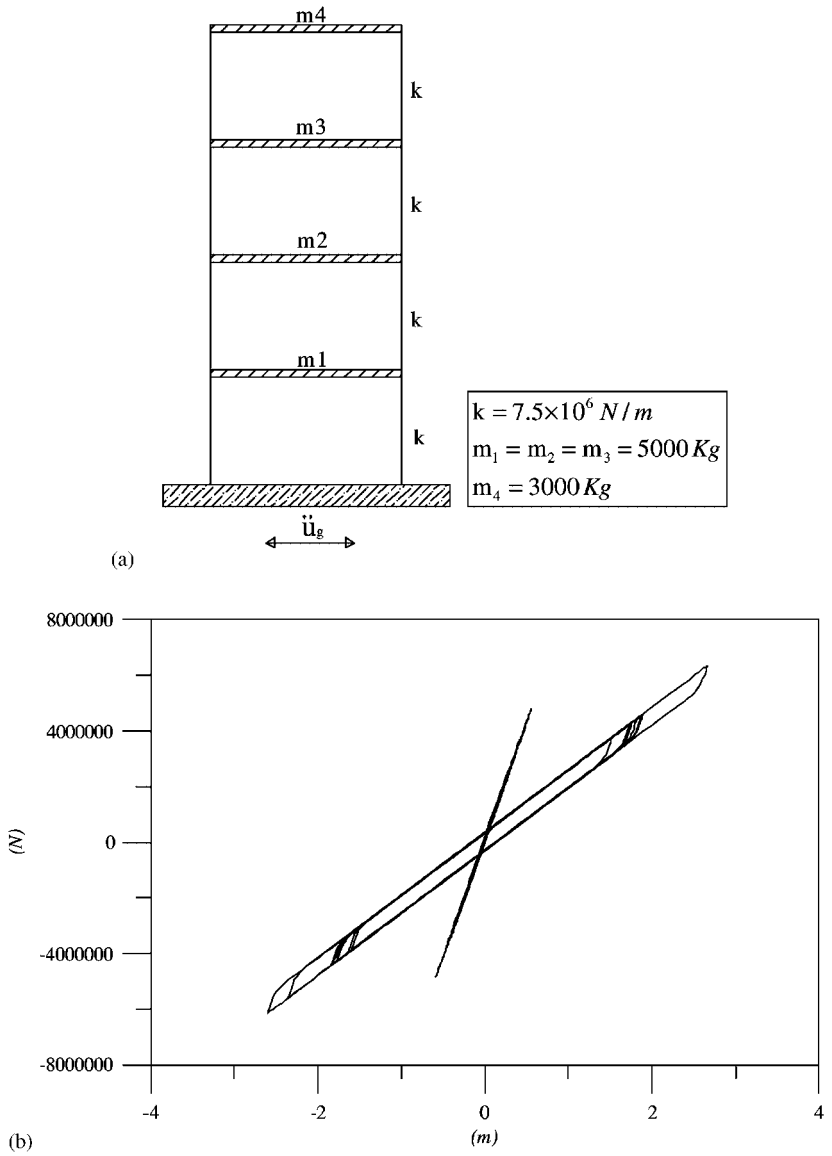

Figure 1. (a) Shear building under analysis; and (b) hysteresis loop pre and post damage.

Figure 1(b) shows the pre and post-damage forms of the hysteresis loop. Two monitoring scenarios are considered. In a first scenario, observations of displacement and velocity are assumed to be available only on the first floor. In the second scenario these same measurements are assumed to be available on both the first and the fourth floors. Two frequencies of measurement are moreover explored in order to ascertain the impact of hardware limitations on the performance of each of these filters. In a first set of trials, it is thus assumed that

measurements are available at every time step, while in a second set, they are assumed to be available once every 20 time steps. In order to proceed with the identification process, a model for the non-linearity must be adopted that is robust enough to account to depict a wide range of potential behaviours. A non-parametric representation of the non-linearity [18] is adopted for the model description in the Kalman filter which results in an equation of motion of the form

$$\mathbf{M}\ddot{\mathbf{u}}(t) + \mathbf{F}(\mathbf{u}, \dot{\mathbf{u}}) = -\mathbf{M}\boldsymbol{\tau}\ddot{u}_g(t) \tag{30}$$

where $\mathbf{F}(\mathbf{u}, \dot{\mathbf{u}})$ is the non-linear restoring force, with its elements described as

$$\begin{aligned}\mathbf{F}_i(\mathbf{u}\dot{\mathbf{u}}) = {} & a_i(u_i - u_{i-1}) + a_{i+1}(u_i - u_{i+1}) + b_i(u_i - u_{i-1})^2 + b_{i+1}(u_i - u_{i+1})^2 \\ & + c_i(\dot{u}_i - \dot{u}_{i-1}) + c_{i+1}(\dot{u}_i - \dot{u}_{i+1}) \\ & + d_i(u_i - u_{i-1})(\dot{u}_i - \dot{u}_{i-1}) + d_{i+1}(u_i - u_{i+1})(\dot{u}_i - \dot{u}_{i+})\end{aligned} \tag{31}$$

where i refers to the floor, a, b, c and d are the unknown parameters to be identified. It is supposed that the true system is essentially linear in the neighbourhood of the origin so that the initial guess for the parameters can be accurately obtained from a linearized model. A zero-mean Gaussian white noise is assumed to perturb the model and the measurements with values equal, respectively, to 0.5 and 0.001. At first both the ExKF and EnKF are applied assuming measurements at the first and fourth floors and an interval between two observations equal to one time step ($\Delta t = 0.005$ s). Figure 2 shows the corresponding results. The vertical line in this and all subsequent figures, at around 5 s, indicates the instant of damage initiation. The top plot shows the estimated states for the first floor, while the bottom plot shows the states for the fourth floor. The two plots in Figure 2 show that both filters are able to detect the state of the system. Results for the other floors show perfect detection and hence support this conclusion. Both ExKF and EnKF are able to describe the time and the location of damage as indicated in the identified evolution of the unknown model parameters in Figure 3. Each plot in this figure shows the evolution of the coefficients appearing in the non-parametric model (Equation (31)) for the non-linear restoring force at a given floor. It is clear from investigating the parameters that the main change is concentrated in the first floor at a time equal to 5 s (in the displacement and velocity results a vertical line represent the instant of damage). It is also clear from this

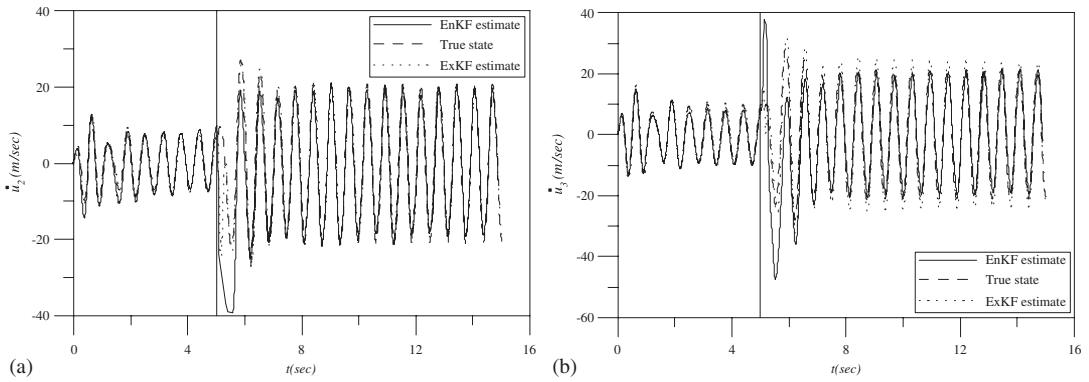

Figure 2. (a) Estimate of the second floor velocity (first and fourth floor observed, $\Delta s = 1$ time steps); and (b) estimate of the third floor velocity (first and fourth floor observed, $\Delta s = 1$ time steps).

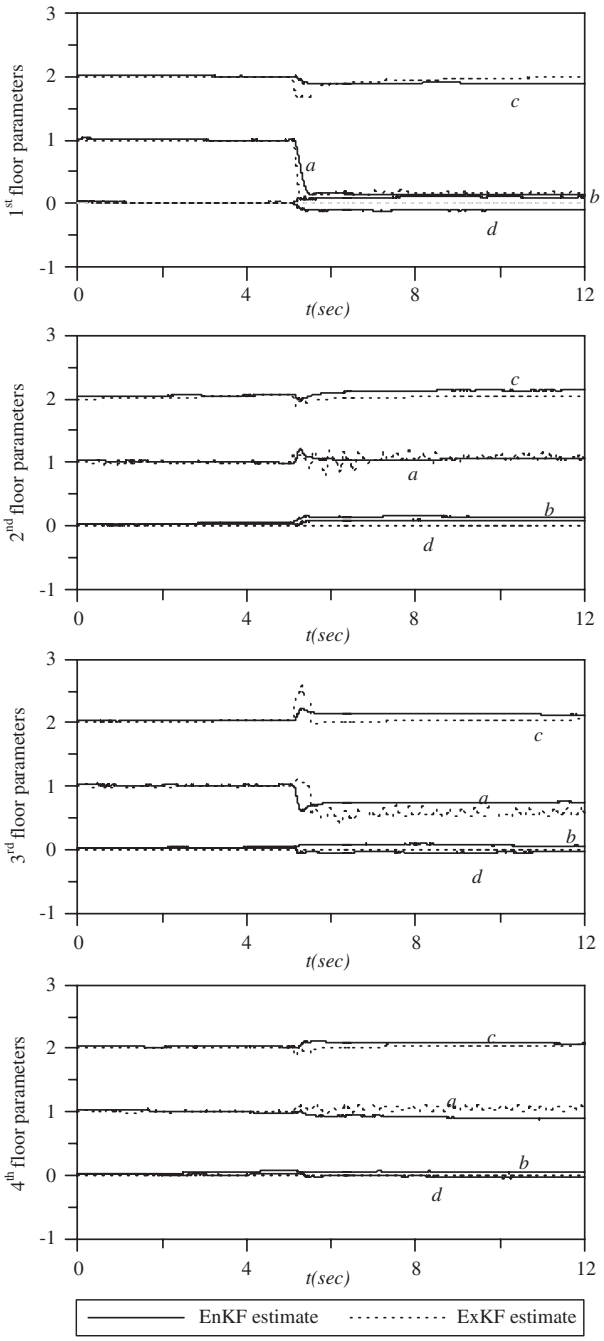

Figure 3. Estimate of the model parameters for each floor (first and fourth floor observed, $\Delta s = 1$ time steps).

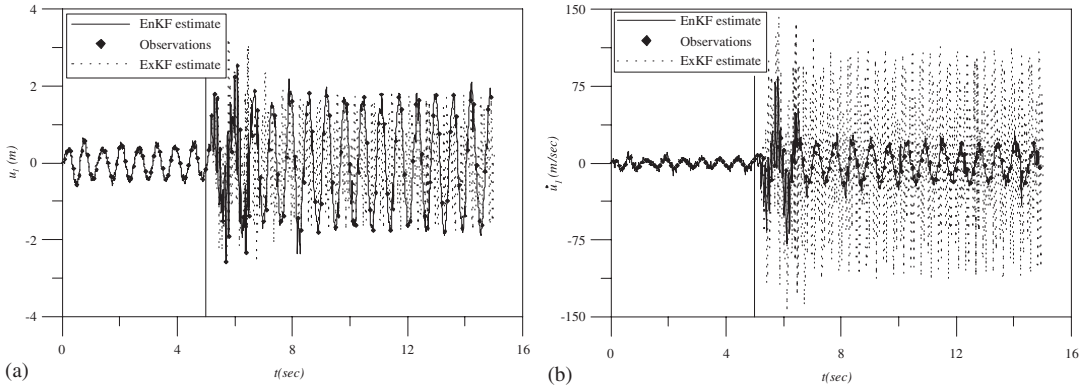

Figure 4. (a) Estimate of the first floor displacement (first floor observed, $\Delta s = 20$ time steps); and (b) estimate of the first floor velocity (first floor observed, $\Delta s = 20$ time steps).

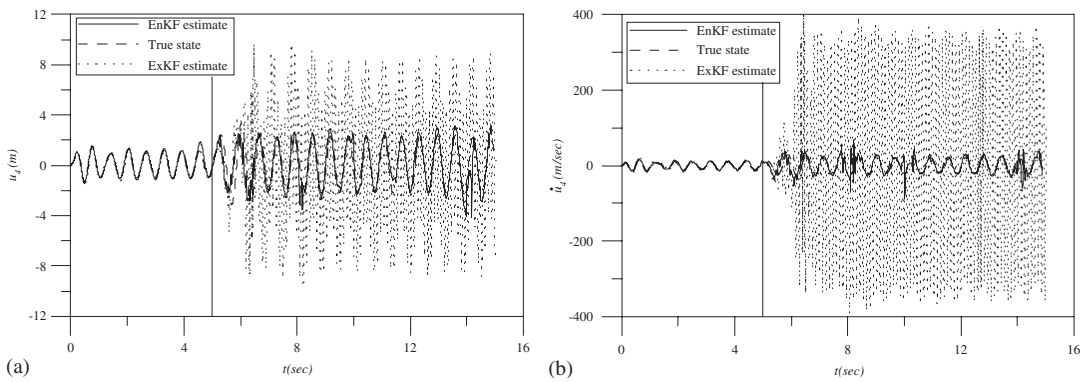

Figure 5. (a) Estimate of the fourth floor displacement (first floor observed, $\Delta s = 20$ time steps); and (b) estimate of the fourth floor velocity (first floor observed, $\Delta s = 20$ time steps).

figure that the non-parametric model adopted here is sensitive to variations in the localized hysteretic behaviour.

The second case considered involves an interval between two successive observations equal to twenty time steps ($\Delta s = 20$), when only displacement of the first floor is used in the identification. Such time lag may be induced by hardware and processing limitations. Figures 4–6 show the corresponding results. Figure 4 shows the tracked displacement and velocity of the first floor, while Figure 5 shows those of the fourth floor. It is readily noted that though before the damage both filters perform adequately, after the damage only the EnKF is able to continue tracking. The ExKF is not able to converge to the damaged state (Figures 4 and 5) and, as a consequence, wrong values for the parameters are obtained (Figure 6). This can be attributed to the better robustness of the EnKF with respect to severe non-linearities.

The second example investigates the same structural system as above, which is now subjected to a base motion specified by a time series consistent with the El-Centro earthquake. Only the EnKF is applied to this problem. It is assumed that only observations of displacement and

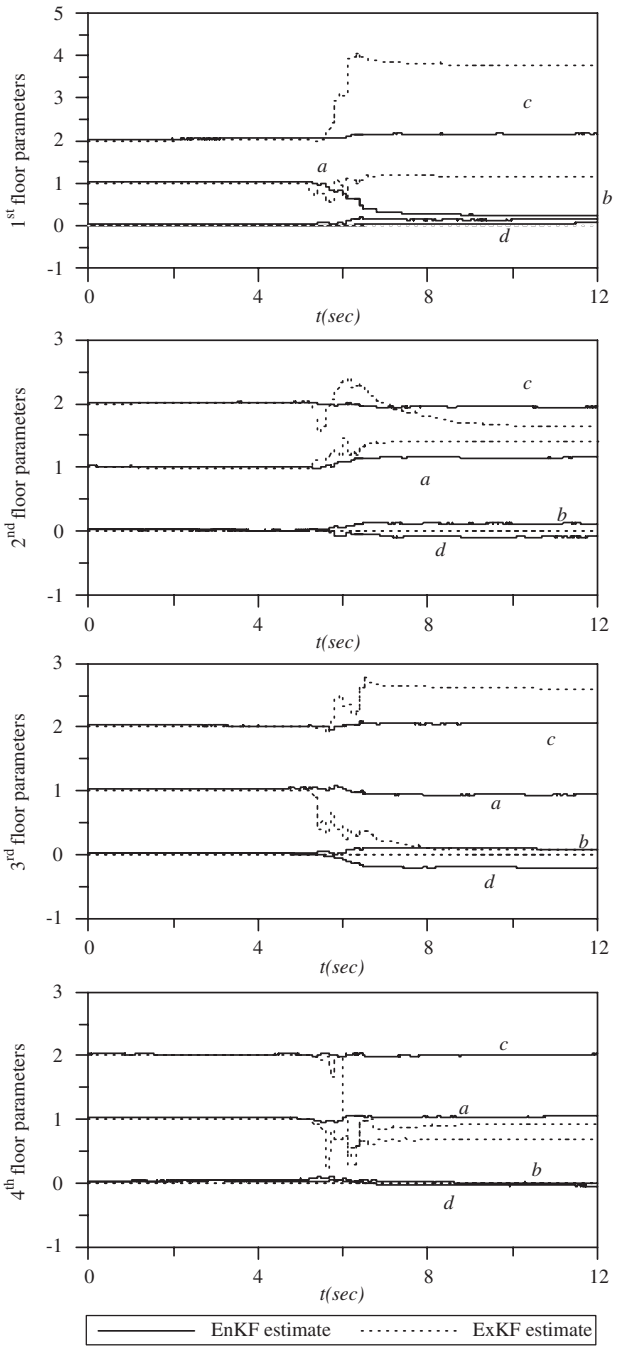

Figure 6. Estimate of the model parameters for each floor (first floor observed, $\Delta s = 20$ time steps).

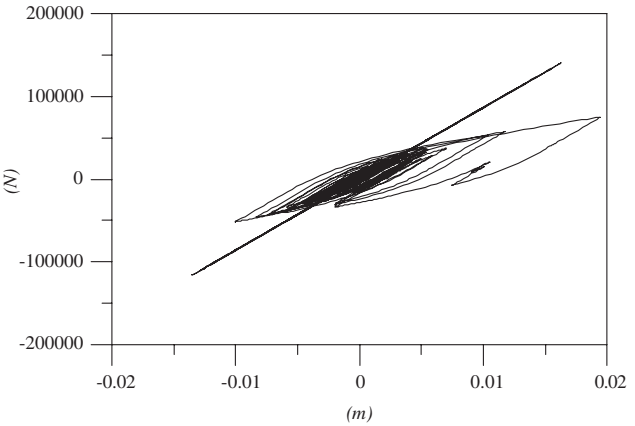

Figure 7. Hysteresis loop pre and post damage.

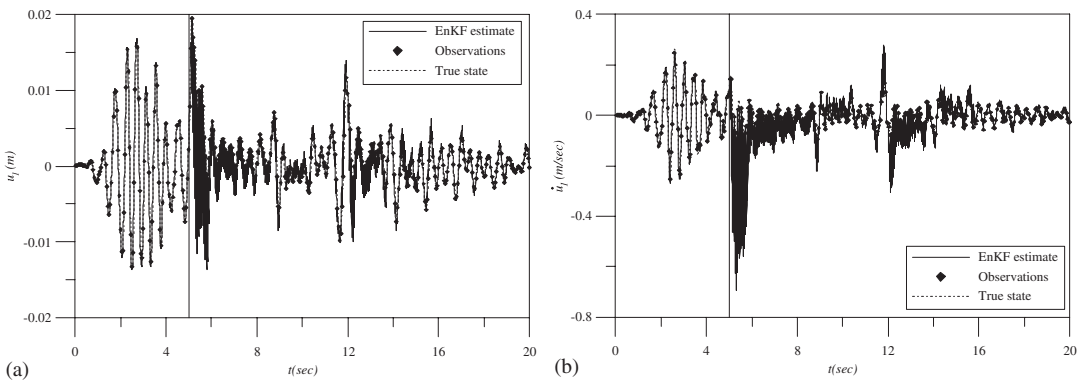

Figure 8. (a) Estimate of the first floor displacement (first floor observed, $\Delta s = 20$ time steps); and (b) estimate of the first floor velocity (first floor observed, $\Delta s = 20$ time steps).

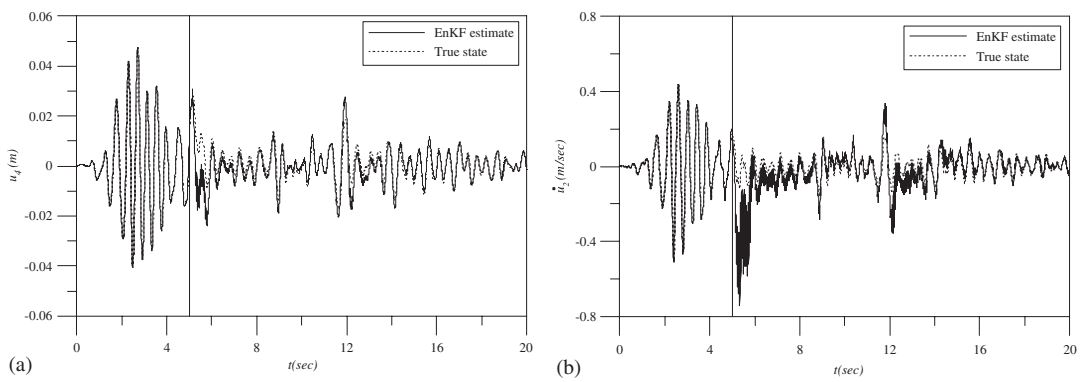

Figure 9. (a) Estimate of the fourth floor displacement (first floor observed, $\Delta s = 20$ time steps); and (b) estimate of the fourth floor velocity (first floor observed, $\Delta s = 20$ time steps).

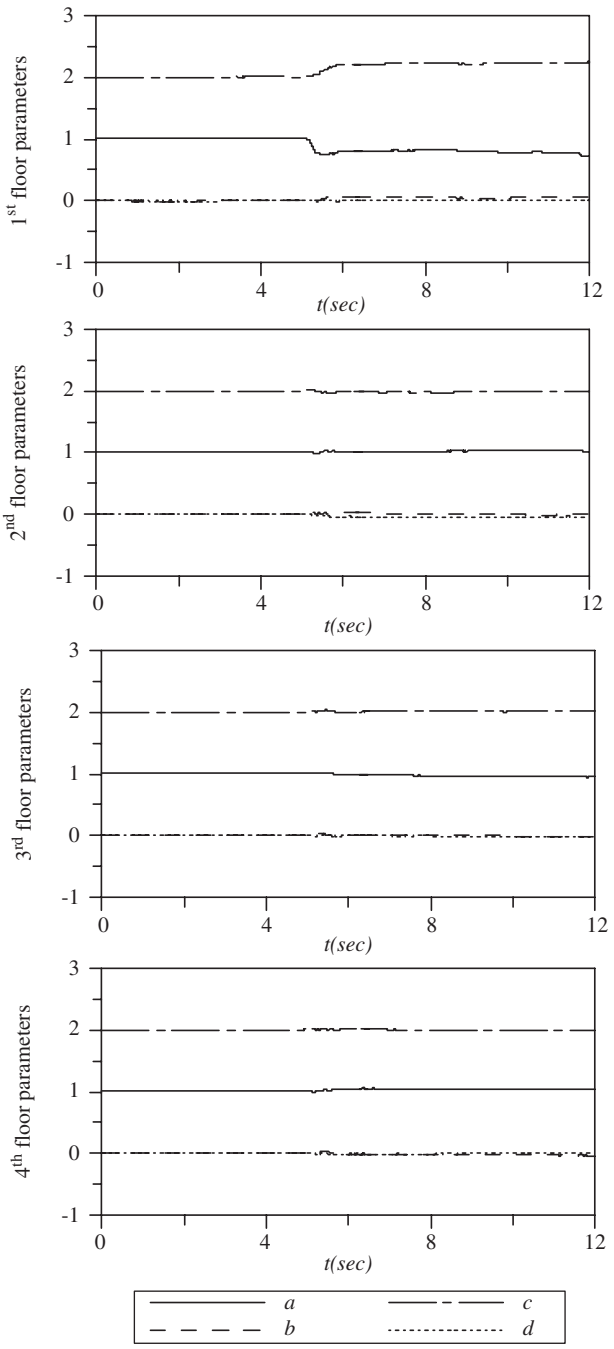

Figure 10. Estimate of the model parameters for each floor (first floor observed, $\Delta s = 20$ time steps).

velocity from the first floor are available. It is also assumed that measurements are collected once every 20 time steps. The noise signals perturbing the model and the measurements, both have zero-mean and their RMS is equal, respectively, to 0.005 and 0.0001. Both damage and observations are concentrated on the first floor, with the damage occurring at 5 s. Figure 7 describe the evolution of hysteretic restoring force related to the first floor. Figures 8 and 9 describe the tracking of displacement and velocity for the first and the fourth floor, respectively. These figures compare the estimated state using the ensemble Kalman filter with the perturbed observed state (which include measurement noise) for the first floor and with the real solution for the other floors. Excellent match is observed. Figure 10 describes the evolution of the unknown parameters identified by the EnKF for each floor. It is again readily noted that the damage is perfectly detected at 5 s and on the first floor. The non-parametric model, coupled with the EnKF seems to provide a superb capability for isolating the damage both in space and time.

5. CONCLUSION

The EnKF is introduced to the area of structural health monitoring and its performance assessed in relation to the ExKF, both for state and for parameter estimation. Although the EnKF has been applied extensively in recent years in various geophysical areas, its application to structural health monitoring merits some consideration. Specifically, issues of time delay and space-time localization of peculiar events are more severe in the present context and present a challenge that the EnKF seems to tackle quite well. While issues of numerical efficiency may be a bottleneck at this stage, it is noted that the EnKF algorithm lends itself very readily to coarse-grained parallelization and stands to benefit significantly from further advances in computer technology.

Also worth noting in the present work, is the robustness with which a non-parametric model for non-linearities has permitted the EnKF to identify damage and track dynamical states beyond its inception. This point is quite significant as in most practical situations, models of non-linear behaviour are not well understood or known *a priori*. Even if such models were known, the performance of the surrogate non-parametric model permits the efficient characterization of both state and parameters, which will greatly facilitate related activities such as structural control.

ACKNOWLEDGEMENTS

The financial support of NSF under grant number DMS-0512231 is gratefully acknowledged.

REFERENCES

1. Ghanem R, Shinozuka M. Structural systems identification i: theory. *Journal of Engineering Mechanics* 1995; **121**:255–264.
2. Lus H, Betti R, Longman R. Obtaining refined first-order predictive models of linear structural systems. *Earthquake Engineering and Structural Dynamics* 2002; **31**:1413–1440.
3. Zhang H, Foliente G, Yang Y, Ma F. Parameter identification of inelastic structures under dynamic loads. *Earthquake Engineering and Structural Dynamics* 2002; **31**:1113–1130.

4. Koh CG, Shankar K. Substructural identification method without interface measurement. *Journal of Engineering Mechanics* 2003; **129**:769–776.
5. Franco G, Betti R, Lus S. Identification of structural systems using an evolutionary strategy. *Journal of Engineering Mechanics* 2003; **130**:1125–1139.
6. Furukawa T, Ito M, Izawa K, Noori M. System identification of base-isolated building using seismic response data. *Journal of Engineering Mechanics* 2005; **131**:268–275.
7. Smyth A, Masri S, Caughey TK, Hunter N. Surveillance of mechanical systems on the basis of vibration signature analysis. *Journal of Applied Mechanics* 2000; **67**:540–551.
8. Loh C, Lin C-Y, Huang CC. Time domain identification of frames under earthquake loadings. *Journal of Engineering Mechanics* 2000; **127**:693–703.
9. Yang J, Lin S. Identification of parametric variations of structures based on least squares estimation and adaptive tracking technique. *Journal of Engineering Mechanics* 2005; **131**:290–298.
10. Chui C, Chen G. *Kalman Filtering with Real-Time Application*. Springer: Berlin, 1987.
11. Corigliano A, Mariani S. Parameter identification in explicit structural dynamics: performance of the extended kalman filter. *Computer Methods in Applied Mechanics and Engineering* 2004; **193**:3807–3835.
12. Ghanem R, Romeo F. A wavelet-based approach for the identification of linear time varying dynamical systems. *Journal of Sound and Vibration* 2000; **234**:555–576.
13. Ching J, Glaser S. Tracking rapidly changing dynamical systems using a non-parametric statistical method based on wavelets. *Earthquake Engineering and Structural Dynamics* 2003; **32**:2377–2406.
14. Evensen G. Sequential data assimilation with a nonlinear quasi-geostrophic model using monte carlo methods to forecast error statistics. *Journal of Geophysical Research* 1994; **99**(C5):10143–10162.
15. Evensen G. The ensemble kalman filter: theoretical formulation and practical implementation. *Ocean Dynamics* 2003; **53**:343–367.
16. Zou Y, Ghanem R. Multiscale data assimilation with the ensemble kalman filter. *SIAM Journal of Multiscale Modeling* 2004; **3**(1):131–150.
17. Zou Y, Ghanem R. Error estimation for the spatial discretization of multiscale bridging models. *SIAM Journal of Multiscale Modeling* 2005; **3**(2):940–956.
18. Masri SF, Caffrey JP, Caughey TK, Smyth AW, Chassiakos AG. Identification of the state equation in complex nonlinear systems. *International Journal of Non-Linear Mechanics* 2004; **39**:1111–1127.
19. Del Modal P. *Feynman-Kac Formulae*; *Genealogical and Interacting Particle Systems with Applications*. Springer: Berlin, 2004.
20. Sadek F, Mehdi B, El-Borgi S, McCormick J, Riley M. An innovative approach for controlling hysteretic structures using static output feedback H_∞ algorithm and stochastic linearization techniques. In *Third World Congress on Structural Control*, Como, Italy, 7–11 April 2002; 1–6.

